CrossMark
click for updates

A Two-Component *para*-Nitrophenol Monooxygenase Initiates a Novel 2-Chloro-4-Nitrophenol Catabolism Pathway in *Rhodococcus imtechensis* RKJ300

Jun Min,[a] Jun-Jie Zhang,[a] Ning-Yi Zhou[a,b]

Key Laboratory of Agricultural and Environmental Microbiology, Wuhan Institute of Virology, Chinese Academy of Sciences, Wuhan, China[a]; State Key Laboratory of Microbial Metabolism & School of Life Sciences and Biotechnology, Shanghai Jiao Tong University, Shanghai, China[b]

Rhodococcus imtechensis RKJ300 (DSM 45091) grows on 2-chloro-4-nitrophenol (2C4NP) and *para*-nitrophenol (PNP) as the sole carbon and nitrogen sources. In this study, by genetic and biochemical analyses, a novel 2C4NP catabolic pathway different from those of all other 2C4NP utilizers was identified with hydroxyquinol (hydroxy-1,4-hydroquinone or 1,2,4-benzenetriol [BT]) as the ring cleavage substrate. Real-time quantitative PCR analysis indicated that the *pnp* cluster located in three operons is likely involved in the catabolism of both 2C4NP and PNP. The oxygenase component (PnpA1) and reductase component (PnpA2) of the two-component PNP monooxygenase were expressed and purified to homogeneity, respectively. The identification of chlorohydroquinone (CHQ) and BT during 2C4NP degradation catalyzed by PnpA1A2 indicated that PnpA1A2 catalyzes the sequential denitration and dechlorination of 2C4NP to BT and catalyzes the conversion of PNP to BT. Genetic analyses revealed that *pnpA1* plays an essential role in both 2C4NP and PNP degradations by gene knockout and complementation. In addition to catalyzing the oxidation of CHQ to BT, PnpA1A2 was also found to be able to catalyze the hydroxylation of hydroquinone (HQ) to BT, revealing the probable fate of HQ that remains unclear in PNP catabolism by Gram-positive bacteria. This study fills a gap in our knowledge of the 2C4NP degradation mechanism in Gram-positive bacteria and also enhances our understanding of the genetic and biochemical diversity of 2C4NP catabolism.

Chloronitrophenols, such as 2-chloro-4-nitrophenol (2C4NP), 4-chloro-2-nitrophenol (4C2NP), and 2-chloro-5-nitrophenol (2C5NP), with high toxicity to human beings and animals have been widely used in the pharmaceutical, agricultural, and chemical industries (1). The natural formation of chloronitrophenols is rare, and most of these compounds in the environment result from anthropogenic activity. Apparently, the introduction of chloronitrophenols into the environment has selected microorganisms to develop the ability to degrade these compounds. So far, several strains able to degrade chloronitrophenols have been isolated, including the 2C4NP-degrading strains *Burkholderia* sp. strain SJ98 (2), *Burkholderia* sp. strain RKJ800 (3), *Rhodococcus imtechensis* RKJ300 (4), and *Arthrobacter* sp. strain SJCon (5), the 4C2NP-degrading strain *Exiguobacterium* sp. strain PMA (6), and the 2C5NP-degrading strain *Ralstonia eutropha* JMP134 (7).

Structurally, chloronitrophenols are chemical analogs of nitrophenols. The microbial degradation of nitrophenols has been extensively investigated at genetic and biochemical levels (8–13). In contrast to nitrophenols, chloronitrophenols are more resistant to microbial degradation due to the simultaneous existence of electron-withdrawing chloro and nitro groups, and the knowledge of their microbial degradation is thus very limited. Previously, the partially purified enzymes involved in *meta*-nitrophenol catabolism were reported to be able to catalyze 2C5NP transformation in *Ralstonia eutropha* JMP134 (7). In the case of 2C4NP degradation, strains RKJ300 (4) and RKJ800 (3) were reported to degrade 2C4NP via the hydroquinone (HQ) pathway, whereas strains SJ98 (14) and SJCon (5) degraded 2C4NP with chlorohydroquinone (CHQ) as the ring cleavage substrate. In particular, the enzymes encoded by *pnpABCDEF* were recently proved to be involved in 2C4NP catabolism in Gram-negative *Burkholderia* sp. strain SJ98 (14). However, no investigation has been reported at the genetic

and enzymatic levels for the 2C4NP catabolism in Gram-positive utilizers *Arthrobacter* sp. strain SJCon (5) and *Rhodococcus imtechensis* RKJ300 (4).

In this study, a novel 2C4NP catabolic pathway via hydroxyquinol (hydroxy-1,4-hydroquinone or 1,2,4-benzenetriol [BT]), which is significantly different from those of other 2C4NP utilizers, was characterized at biochemical and genetic levels in strain RKJ300. To our surprise, BT was identified as the ring cleavage substrate during 2C4NP degradation in this strain, rather than HQ as previously proposed (4). On the other hand, the two-component (TC) *para*-nitrophenol (PNP) monooxygenase PnpA1A2 in this strain was found to be able to catalyze the sequential denitration and dechlorination of 2C4NP to BT, and *pnpA1* is essential for strain RKJ300 to utilize 2C4NP and PNP. This study fills a gap in terms of our knowledge of the microbial degradation mechanism of 2C4NP in the Gram-positive bacteria and should also enhance our understanding of the genetic and biochemical diversity of microbial catabolism of 2C4NP.

TABLE 1 Bacterial strains and plasmids used in this study

Strain or plasmid	Relevant genotype or characteristic(s)[a]	Source or reference
Strains		
Rhodococcus imtechensis		
RKJ300	PNP and 2C4NP utilizer, wild type	4
RKJ300Δ*pnpA1*	RKJ300 mutant with *pnpA1* gene deleted	This study
RKJ300Δ*pnpA1* [pRESQ-*pnpA1*]	*pnpA1* gene complemented by pRESQ-*pnpA1* in RKJ300Δ*pnpA1*	This study
Escherichia coli		
DH5α	*supE44 lacU169* (φ80 *lacZ*ΔM15) *recA1 endA1 hsdR17 thi-1 gyrA96 relA1*	Novagen
Rosetta(DE3)/pLysS	F⁻ *ompT hsdS*(r_B^- m_B^+) *gal dcm lacY1*(DE3)/pLysSRARE (Cm^r)	Novagen
S17-1	*thi pro hsdR hsdM$^+$ recA* R⁻ M$^+$ RP4-2-Tc::Mu-Km::Tn7	30
Plasmids		
pET-28a	Expression vector, Kan^r	Novagen
pXMJ19	Source of chloramphenicol resistance gene	28
pK18*mobsacB*	Gene replacement vector derived from plasmid pK18; Mob$^+$ *sacB$^+$* Kan^r	29
pRESQ	*Rhodococcus-E. coli* shuttle vector, Kan^r	32
pET-*pnpA1*	NdeI-HindIII fragment containing *pnpA1* inserted into pET-28a	This study
pET-*pnpA2*	NdeI-HindIII fragment containing *pnpA2* inserted into pET-28a	This study
pK18*mobsacB*-*pnpA1*	*pnpA1* gene knockout vector containing 2 DNA fragments homologous to upstream and downstream regions of *pnpA1* and chloramphenicol resistance gene	This study
pRESQ-*pnpA1*	*pnpA1* gene complementation vector made by fusing *pnpA1*, including its native promoter, into BglII restriction site of pRESQ	This study

[a] Cm, chloramphenicol; Kan, kanamycin.

MATERIALS AND METHODS

Bacterial strains, plasmids, primers, media, and culture conditions. The bacterial strains and plasmids used in this study are described in Table 1, and the primers used are listed in Table 2. *Rhodococcus* strains were grown at 30°C in lysogeny broth (LB) medium or minimal medium (MM) (15) supplemented with substrates (0.2% yeast extract was added to enhance the biomass when cultures were prepared for biotransformation assays). *Escherichia coli* strains were grown in LB at 37°C. Kanamycin (50 μg/ml) or chloramphenicol (34 μg/ml) was added to the medium as necessary. All reagents were purchased from Sigma Chemical Co. (St. Louis, MO) or Fluka Chemical Co. (Buchs, Switzerland).

Biotransformation and identification of intermediates. Biotransformation was performed as described previously (16) with minor modifications. RKJ300 strains were grown on MM with 0.2% yeast extract to an optical density at 600 nm (OD$_{600}$) of 0.3 and then induced by 0.3 mM 2C4NP or PNP for 8 h. Cells were harvested, washed twice, and diluted to an OD$_{600}$ of 2.0 with phosphate buffer (20 mM, pH 7.5) before 0.2 mM substrate (2C4NP or PNP) was added. Then 0.5-ml samples were withdrawn at regular intervals before being mixed with an equal volume of methanol and vortexed rigorously for 10 min. Each sample was then centrifuged at 15,000 × g at 4°C for 20 min before the supernatant was collected for high-performance liquid chromatography (HPLC) analysis. In order to accumulate the intermediates before ring cleavage, 1 mM 2,2′-dipyridyl was added to the biotransformation mixtures. For gas chromatography-mass spectrometry (GC-MS) analysis of the intermediates, the phenolic compounds in the supernatant were acetylated as described previously (17).

Analytical methods. HPLC analysis was performed as described previously (18). The authentic CHQ, hydroquinone (HQ), and BT had retention times of 16.5, 10.8, and 8.1 min, respectively. The conditions of GC-MS analysis were the same as those described previously (9), except the mass spectrometer was recorded in the range from *m/z* 20 to *m/z* 300. Under these conditions, acetylated derivatives of authentic CHQ, HQ, and BT had GC retention times of 16.66, 15.00, and 19.06 min, respectively. The acetylated derivatives of the intermediates were identified using an NIST98 MS data library, based on comparisons of the GC retention times and mass spectra with those of the derivatives of authentic compounds.

RNA preparation and transcription analysis. Total RNA from strain RKJ300 was isolated using the hot phenol method (19) and reverse transcribed into cDNA using a PrimeScript RT reagent kit (TaKaRa, Dalian, China). Reverse transcription (RT)-PCR was carried out with the primers listed in Table 2. Real-time quantitative PCR (RT-qPCR) was performed on a CFX Connect real-time PCR detection system (Bio-Rad, Hercules, CA) in 25-μl reaction volumes using iQ SYBR green supermix (Bio-Rad) and the primers described in Table 2. All samples were run in triplicate in three independent experiments. Relative expression levels were estimated using the cycle threshold ($2^{-\Delta\Delta C_T}$) method, and the 16S rRNA gene was used as a reference for normalization (20).

Protein expression and purification. *pnpA1* and *pnpA2* amplified by PCR with primers in Table 2 from genomic DNA of strain RKJ300 were cloned into pET-28a to obtain the expression constructs listed in Table 1. The plasmids were then transformed into *E. coli* Rosetta(DE3)/pLysS for protein expression and purification as described previously (21).

Enzyme assays. The NAD(P)H-oxidizing activities of H$_6$-PnpA2 were measured as described previously (18). The oxidizing activity toward phenolic compounds (2C4NP, PNP, CHQ, and HQ) of PnpA1A2 was measured as described previously (22) with minor modification. The reaction mixture contained 50 mM Tris-HCl buffer (pH 7.5), 0.2 mM NADH, 0.02 mM flavin adenine dinucleotide (FAD), purified H$_6$-PnpA2 (0.1 to 2 μg), and purified H$_6$-PnpA1 (15 to 60 μg) in a final volume of 1 ml, and the assay was initiated by addition of substrates. The molar extinction coefficients for NAD(P)H, PNP, and 2C4NP were 6,220 M^{-1} cm^{-1} at 340 nm (23), 7,000 M^{-1} cm^{-1} at 420 nm (24), and 14,580 M^{-1} cm^{-1} at 405 nm (25), respectively. The products of the purified PnpA1A2-catalyzed reaction were identified by HPLC (18) and GC-MS (17). For the quantification analysis of the products, 1 mM ascorbic acid (26) was added as a reducing reagent to minimize the autoxidation of the products HQ, CHQ, and BT.

In the kinetic assays of H$_6$-PnpA2, specific activities of PnpA2 for NADH were measured at 7 concentrations of NADH (10 to 100 μM) in the presence of 20 μM FAD (for the determination of the kinetic param-

TABLE 2 Primers used in this study

Primer	Sequence (5′→3′)[a]	Purpose
pnpA1-F	AGGCAC<u>CATATG</u>AGGACAGGACAGCAGTATC	Amplification of *pnpA1* gene for expression
pnpA1-R	TTT<u>AAGCTT</u>TCAGACCTTCTCGGTCTCC	
pnpA2-F	AGGCAC<u>CATATG</u>TTGGAGGATCCGATGAAAC	Amplification of *pnpA2* gene for expression
pnpA2-R	TTT<u>AAGCTT</u>TCAGTGGGGGGAAACTGC	
RTA1-F	GAACAGAACGACCAGGGAATC	Amplification of 565 bp of *pnpA* by RT-PCR
RTA1-R	CGTAGATGTTGTTGGGCTTG	
RTA2-F	GCCCTTGGACAAAGCCGAAT	Amplification of 397 bp of *pnpA2* by RT-PCR
RTA2-R	GACCTCGGCGACGAAAATG	
RTB-F	TGCGTTTATCCGTGAAGTGC	Amplification of 347 bp of *pnpB* by RT-PCR
RTB-R	CGTCGTTCTGCCACACCTC	
RTC-F	GCGGAGGAGAGAGCGAATC	Amplification of 656 bp of *pnpC* by RT-PCR
RTC-R	CCATCTACGGGCTCACCAG	
RTA2A1-F	CAAGTTCGCCGATGTAGCC	Amplification of 565 bp of *pnpA2*-*pnpA1*-spanning region
RTA2A1-R	AGATACCTCCCTGGAAGTGCC	
RTA1B-F	GCCGAGGTGGAGAAGAACT	Amplification of 363 bp of *pnpA1*-*pnpB*-spanning region
RTA1B-R	GCACTTCACGGATAAACGC	
RTRA2-F	CGGCACATCACTCGTCAGC	Amplification of 749 bp of *pnpR*-*pnpA2*-spanning region
RTRA2-R	TGAGCCAGGGACGCTTGAT	
RTCR-F	GCTGGTGAGCCCGTAGATG	Amplification of 701 bp of *pnpC*-*pnpR*-spanning region
RTCR-R	CTCGGTGACACTTCGCATG	
RTq16S-F	ATGGCTGAGGGTGGAAAGG	Amplification of 112-bp fragment of 16S rDNA for RT-qPCR
RTq16S-R	TCACCCTCTCAGGTCGGC	
RTq-*pnpA1*-F	GGAACAGAACGACCAGGGAATC	Amplification of 162-bp fragment of *pnpA1* for RT-qPCR
RTq-*pnpA1*-R	AGTGAGAGCCCAGGGGTGTT	
RTq-*pnpC*-F	GCCGAGGTGATGAAATGTGAC	Amplification of 163-bp fragment of *pnpC* for RT-qPCR
RTq-*pnpC*-R	GCCGAGGACTGACAAGATTC	
GC-*pnpA1*-F	TACCGAGCTCAGATCCGGGCGCGAGCGTTGAG	Amplification of *pnpA1* for gene complementation
GC-*pnpA1*-R	CGTTACTAGTAGATCTCAGACCTTCTCGGTCTCC	
KO-*pnpA1*u-F	ACATGATTACGAATTCTCGTCGATCCGCCAATTC	Amplification of upstream sequence of *pnpA1* for gene knockout
KO-*pnpA1*u-R	AACTAGTGATGTAATGGAGGAACCTTTCTCTCTCAGTGC	
KO-*pnpA1*d-F	GAAGGAGATATACATTCCCGGCCCGACAGTCCCAGC	Amplification of downstream sequence of *pnpA1* for gene knockout
KO-*pnpA1*d-R	GGCCAGTGCCAAGCTATCTGTTCTGGTGCAAGGACTATG	
KO-*cm*-F	ATTACATCACTAGTTGAAAAG	Amplification of chloramphenicol resistance gene for gene knockout
KO-*cm*-R	ATGTATATCTCCTTCTTAAATCTAG	

[a] Specified restriction sites are underlined.

eters for NADH) or at 7 concentrations of FAD (1 to 20 μM) in the presence of 100 μM NADH (for the determination of the kinetic parameters for FAD). In the case of the kinetic assays of purified PnpA1A2 against 2C4NP or PNP, 7 concentrations of substrates ranging from 1 to 30 μM were used, while the concentrations of NADH and FAD were fixed at 100 and 20 μM, respectively. Data from three independent sets of experiments were fitted to the Michaelis-Menten equation by OriginPro 8 software (OriginLab, MA). The protein concentration was determined by the Bradford method (27) with bovine serum albumin as the standard. One unit of enzyme activity was defined as the amount of enzyme required to catalyze the consumption of 1 μmol of substrate per min at 30°C. Specific activities are expressed as units per milligram of protein.

Gene knockout and complementation. pK18*mobsacB*-*pnpA1* for gene knockout was constructed by fusing the upstream and downstream fragments of the target gene (*pnpA1*) and chloramphenicol resistance gene amplified from pXMJ19 (28) to EcoRI/HindIII-digested pK18*mobsacB* (29) with an In-Fusion HD cloning kit (TaKaRa, Dalian, China) (primers listed in Table 2). The plasmid was then transformed into strain *E. coli* S17-1 (30) before it was conjugated to strain RKJ300 by biparental mating (31). The single-crossover recombinants were screened on an MM agar plate supplemented with 0.3 mM substrate and 34 μg/ml chloramphenicol. The single-crossover recombinants were then replica plated on LB medium containing 10% (wt/vol) sucrose. After 3 days of growth at 30°C, individual colonies were plated on a kanamycin-containing LB
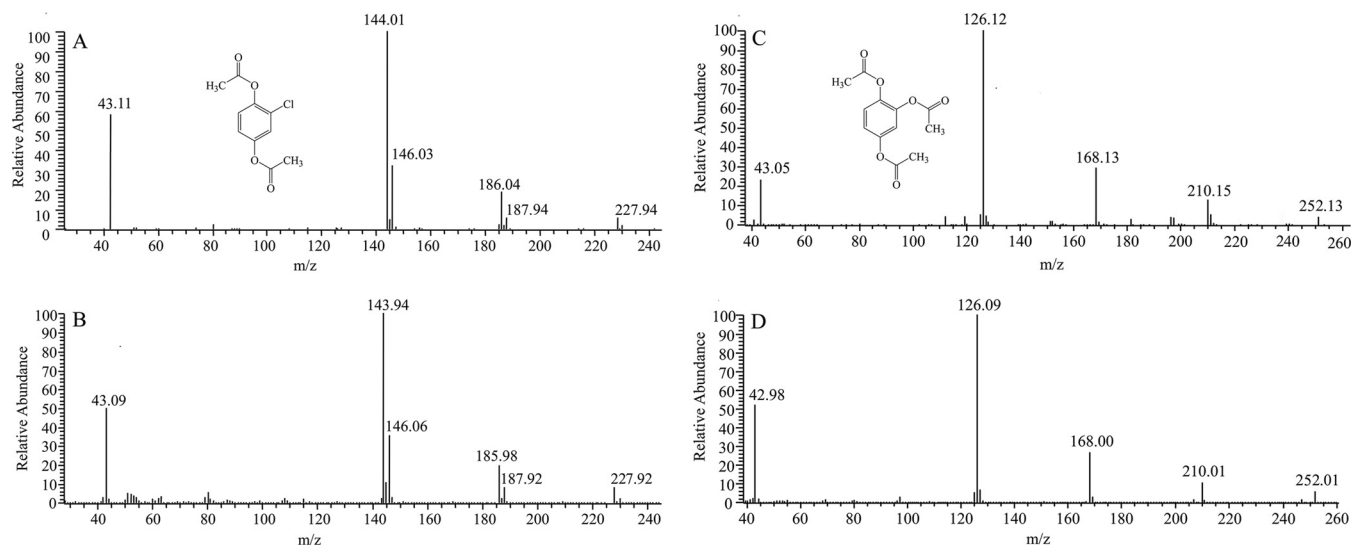
FIG 1 Mass spectra of the acetylated derivatives of the intermediates during 2C4NP degradation by *R. imtechensis* RKJ300. (A) Mass spectrum of the acetylated derivative of authentic CHQ. (B) Mass spectrum of the GC peak at 16.66 min, identical to that of acetylated CHQ. (C) Mass spectrum of the acetylated derivative of authentic BT. (D) Mass spectrum of the GC peak at 19.06 min, identical to that of acetylated BT.

plate as well as chloramphenicol-containing plate. Finally, PCR analysis against the chloramphenicol-resistant but kanamycin-sensitive colonies was carried out to identify the double-crossover recombinants of RKJ300Δ*pnpA1*. pRESQ-*pnpA1* for gene complementation was constructed by fusing the PCR products of *pnpA1* (including its native promoter) into BglII-digested pRESQ ([32]). The plasmid was then transformed into the competent cells of the RKJ300Δ*pnpA1* strain via electro-transformation ([33]). The ability of wild-type strain RKJ300 and its derivatives to utilize the substrates was determined by monitoring the growth of cells together with the consumption of the corresponding substrates.

RESULTS

Strain RKJ300 degrades 2C4NP with BT as the ring cleavage substrate. In order to accumulate the intermediates of 2C4NP and PNP degradation, 2,2′-dipyridyl, which has been used to inhibit a number of ferrous-dependent aromatic ring cleavage enzymes ([34–36]), was added to the biotransformation mixtures. Two metabolites with retention times of 16.5 and 8.1 min, respectively, were detected by HPLC analysis during 2C4NP degradation. These two metabolites were identified as CHQ and BT by comparison with the retention times of standard compounds. Furthermore, GC-MS analysis of the acetylated products also detected two compounds, with GC retention times of 16.66 and 19.06 min, respectively. The mass spectrum of the 16.66-min peak (Fig. 1B) was typical for a molecule containing one chlorine and was identified as acetylated CHQ, with the molecular ion peak at *m/z* 228 and its fragments at *m/z* 186 (loss of —COCH$_3$) and at *m/z* 144 (loss of two —COCH$_3$). The peaks at *m/z* 146 (M + 2) and 144 (M$^+$) and their relative intensities are characteristic of a molecule containing one chlorine atom. The relative intensities are consistent with the natural abundance of 76% for ^{35}Cl and 24% for ^{37}Cl. The mass spectrum of the 19.06-min peak (Fig. 1D) indicated that the compound contained no chlorine atom. It was identified as acetylated BT, with the molecular ion peak at *m/z* 252 and its fragments at *m/z* 210 (loss of —COCH$_3$), *m/z* 168 (loss of two —COCH$_3$'s), and *m/z* 126 (loss of all three —COCH$_3$'s). The identity of the two intermediates as CHQ and BT was further

confirmed by comparison with GC-MS analysis of the acetylated authentic compounds (Fig. 1A and C). Similarly, acetylated derivatives of HQ (with a GC retention time of 15.00 min) and BT were captured when the intermediates were acetylated during PNP degradation (see Fig. S1 in the supplemental material). On the basis of this initial characterization, strain RKJ300 was proposed to degrade both 2C4NP and PNP via the typical BT pathway.

2C4NP degradation in strain RKJ300 is induced by 2C4NP or PNP. Since BT was identified as the ring cleavage substrate for both 2C4NP and PNP degradation by strain RKJ300, whole-cell biotransformation was performed in order to investigate whether the same enzymes catalyze the catabolism of 2C4NP and PNP. The uninduced cells of strain RKJ300 exhibited negligible activity for 2C4NP and PNP. However, either 2C4NP- or PNP-induced cells of strain RKJ300 have the ability to degrade both 2C4NP and PNP rapidly (Fig. 2). This finding indicated that the same set of enzymes were likely involved in both 2C4NP and PNP catabolism and induced by these two substrates. Interestingly, although CHQ and HQ were detected, respectively, during 2C4NP and PNP degradation, 2C4NP-induced cells of strain RKJ300 showed an evidently lower rate of conversion of CHQ (approximately 4.3 μM h^{-1} OD$_{600}$ cell^{-1}) than the cells converting 2C4NP (100 μM h^{-1} OD$_{600}$ cell^{-1}), and PNP-induced cells also exhibited an evidently lower rate of conversion of HQ (approximately 3 μM h^{-1} OD$_{600}$ cell^{-1}) than cells converting PNP (150 μM h^{-1} OD$_{600}$ cell^{-1}). However, both 2C4NP-induced strain RKJ300 and PNP-induced RKJ300 degraded 0.2 mM BT completely in 1 h, similar to the conversion rates for 2C4NP and PNP (shown in Fig. 2). This further confirmed that BT was the ring cleavage substrate in both 2C4NP and PNP catabolism in strain RKJ300, apart from the HPLC and GC-MS identification.

Sequence analyses of 2C4NP catabolic gene cluster. The findings above indicated that the catabolism of 2C4NP and the catabolism of PNP in strain RKJ300 likely share the same set of enzymes, which led us to elucidate their encoding genes. A DNA
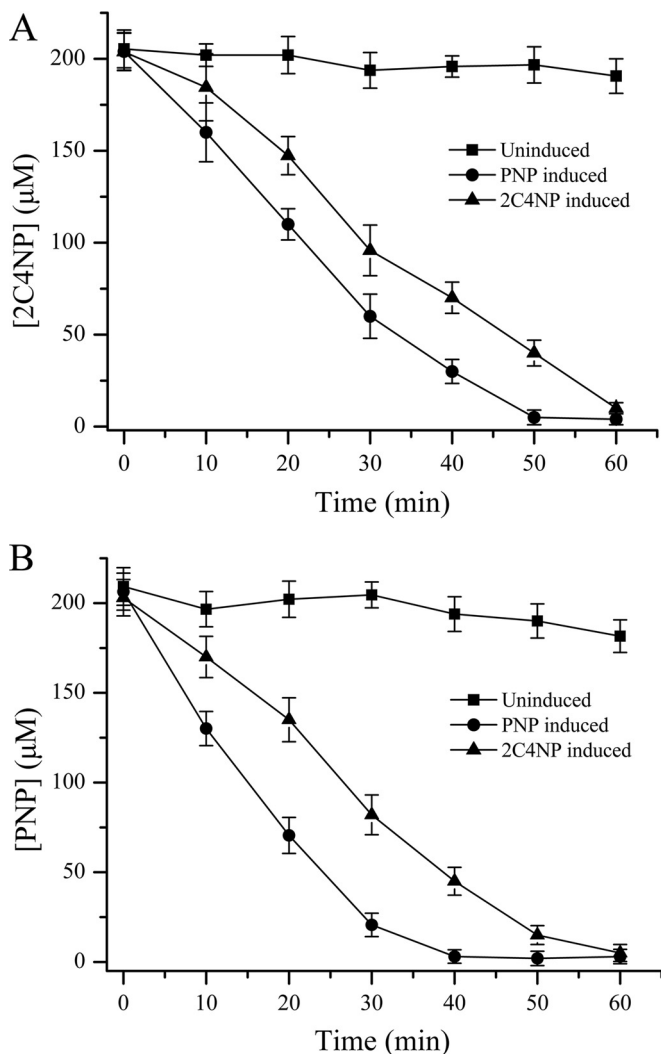
FIG 2 Biotransformation analyses of 2C4NP (A) and PNP (B) degradation by the induced and uninduced cells of *R. imtechensis* RKJ300. The cells were suspended to an OD_{600} of 2.0 with phosphate buffer, and 0.2 mM substrate (2C4NP or PNP) was added. The experiments were performed in triplicate; the results are the average from three independent experiments, and error bars show standard deviations.

fragment with nucleotides from positions 86449 to 92096 of contig 7 (GenBank accession no. AJJH01000007) from the draft genome of strain RKJ300 (37) was designated the *pnp* catabolic cluster, as outlined and annotated in Fig. 3A. Among the products encoded by these genes, PnpA1 and PnpA2 exhibit high degrees of identity to the oxygenase and reductase components, respectively, of the PNP monooxygenase from several Gram-positive PNP utilizers (11, 17, 38), indicating that PnpA1A2 belongs to the phenol 4-monooxygenase group of the two-component flavin-diffusible monooxygenase (TC-FDM) family. PnpB has a high level of identity to NpcC, which was previously reported to catalyze the dioxygenation of BT to maleylacetate during PNP catabolism in *Rhodococcus opacus* SAO101 (11). PnpC appears highly homologous to the known maleylacetate reductase PnpF from *Burkholderia* sp. strain SJ98, which was reported to reduce maleylacetate into β-ketoadipate (14). PnpR was proposed to be an LysR regulatory

protein as it is closely related to NpsR of *Rhodococcus* sp. strain PN1 (38).

***pnp* genes are upregulated in 2C4NP-induced cells of strain RKJ300.** Transcriptional analysis of the *pnp* cluster was carried out in order to investigate whether the enzyme-coding genes were highly transcribed in response to the substrates 2C4NP and PNP. Reverse transcription-PCR was performed with RNA derived from strain RKJ300 with or without the induction of substrates (2C4NP or PNP). The transcription of *pnp* genes was detected only under inducing conditions, and *pnpA2A1B*, *pnpC*, and *pnpR* were proved to be in three different transcriptional operons, as shown in Fig. 3B. In addition, real-time quantitative PCR analysis showed that the transcription levels of *pnpA1* and *pnpC* (each representing their own operons) under the 2C4NP-induced condition were increased dramatically compared to that under the uninduced condition, with 1,878- and 510-fold increases, respectively (Fig. 4). Similarly, the transcription levels of these two genes under PNP-induced condition were 2,804- and 865-fold higher than those under the uninduced condition. This indicated that the enzymes encoded by the *pnp* cluster are likely involved in both 2C4NP catabolism and PNP catabolism in strain RKJ300.

PnpA1A2 catalyzes the monooxygenation of both 2C4NP and PNP to BT. (i) Expression and purification of PnpA1 and PnpA2. Recombinant PnpA1 and PnpA2 were individually overexpressed in *E. coli* Rosetta(DE3)/pLysS as N-terminal His_6-tagged fusion proteins for easy purification. Substantial amounts of soluble and active H_6-PnpA1 and H_6-PnpA2 were synthesized and purified to apparent homogeneity by Ni^{2+}-nitrilotriacetic acid (NTA) affinity chromatography. SDS-PAGE analysis showed that the molecular masses of H_6-PnpA1 and H_6-PnpA2 are approximately 62 and 22 kDa (see Fig. S2 in the supplemental material), respectively, corresponding to the molecular masses deduced from their amino acid sequences.

(ii) Characterization of the reductase component of 2C4NP monooxygenase. As the reductase component of 2C4NP or PNP monooxygenase, NAD(P)H-oxidizing activity of purified H_6-PnpA2 was determined in the presence of FAD or flavin mononucleotide (FMN). Maximal NADH-oxidizing activity was achieved in the presence of FAD with a specific activity of 8.9 U mg^{-1} (defined as 100%). NADH can be replaced by NADPH with 90% efficiency; however, only 25% of activity was present when FAD was replaced by FMN. The kinetic parameter results revealed that the K_m values of H_6-PnpA2 for NADH and FAD were 20.5 ± 2.9 and 3.2 ± 0.4 μM, respectively.

(iii) Characterization of 2C4NP monooxygenase. *E. coli* cells carrying pET-*pnpA1* were still found, by HPLC analysis, to degrade both 2C4NP and PNP, without PnpA2. A possible explanation is that PnpA1 can use free reduced flavins formed by the NADH:FAD oxidoreductase from *E. coli*, and the presence of such flavin reductase was reported in *E. coli* (39). Similar cases were also reported for several other PNP monooxygenases (17, 40). In the assay of purified enzyme, the optimal molar ratio of PnpA2 and PnpA1 of the two-component monooxygenase was determined. The amount of H_6-PnpA2 was increased from 0 to 22.5 nM when the amount of H_6-PnpA1 was kept constant at 1 μM. Negligible 2C4NP or PNP monooxygenation activity was observed when PnpA2 was omitted from the reaction. However, the activity increases rapidly with the addition of PnpA2, and the maximal activity (0.02 U mg^{-1} for 2C4NP and 0.039 U mg^{-1} for PNP) was achieved when PnpA2 was added at 18 nM (Fig. 5). This indicated
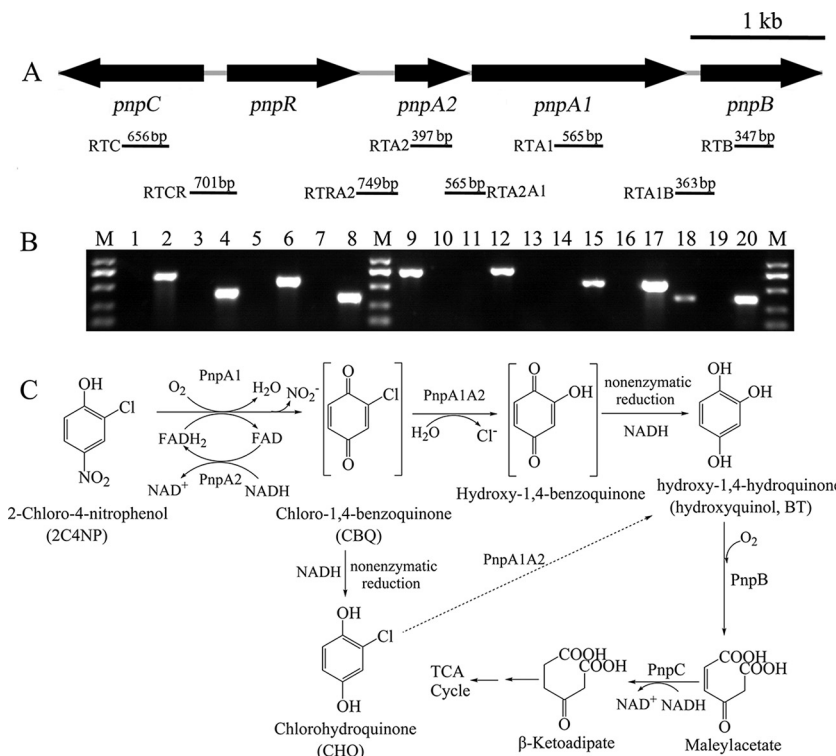
FIG 3 (A) Organization of the *pnp* gene cluster of *R. imtechensis* RKJ300. The black arrows indicate the sizes and directions of transcription of each gene. The locations of primer sets RTC, RTA2, RTA1, RTB, RTCR, RTRA2, RTA2A1, and RTA1B and the DNA fragments amplified for RT-PCR are indicated below. (B) Analysis of *pnpCRA2A1B* transcription by RT-PCR. Total RNAs of strain RKJ300 with or without induction by 2C4NP were prepared for RT-PCR, and reactions performed without RT were used as negative controls. Lanes M, molecular markers of sizes 1,000, 750, 500, 250, and, 100 bp; lanes 2, 4, 6 8, 11, 14, 17, and 20 (template from strain RKJ300 induced by 2C4NP), products amplified using the RTC, RTA2, RTA1, RTB, RTCR, RTRA2, RTA2A1, and RTA1B primer sets, respectively, with products of RT; lanes 1, 3, 5, 7, 10, 13, 16, and 19, corresponding negative controls; lanes 9, 12, 15, and 18 (positive controls with genome DNA as the templates), products amplified using the RTCR, RTRA2, RTA2A1, and RTA1B primer sets, respectively. (C) Proposed pathways for 2C4NP catabolism in *R. imtechensis* RKJ300, together with the catabolic reactions catalyzed by *pnp* gene products. The transformation of CHQ to BT by PnpA1A2 is indicated by a dashed arrow. TCA, tricarboxylic acid.

that the optimal molar ratio of PnpA2 and PnpA1 is about 1:55. Kinetic assays revealed that the K_m values of H_6-PnpA1 for 2C4NP and PNP were 4.4 ± 0.7 and 3.5 ± 0.6 μM, respectively, implying PnpA1 has similar affinities for these two nitrophenol substrates. However, in terms of k_{cat}/K_m values, the catalytic efficiency of

PnpA1 for PNP (k_{cat}/K_m, 0.53 ± 0.03 μM^{-1} min^{-1}) was higher than that for 2C4NP (k_{cat}/K_m, 0.16 ± 0.01 μM^{-1} min^{-1}).

(iv) Identification of the products of 2C4NP and PNP catalyzed by purified PnpA1A2. For the products' identification, 1
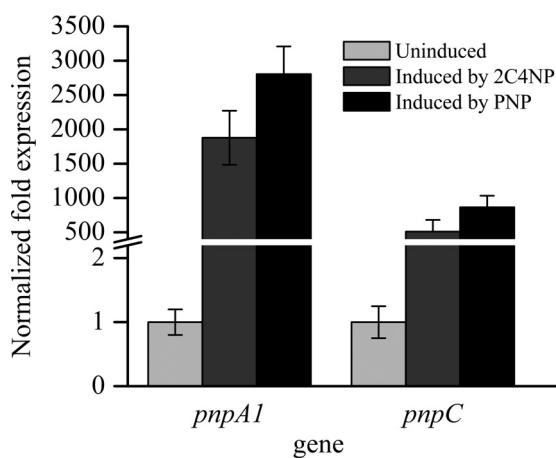
FIG 4 Transcriptional analyses of *pnpA1* and *pnpC* in *R. imtechensis* RKJ300 under induced and uninduced conditions by RT-qPCR. The data are derived from three independent measurements, and error bars indicate standard deviations.
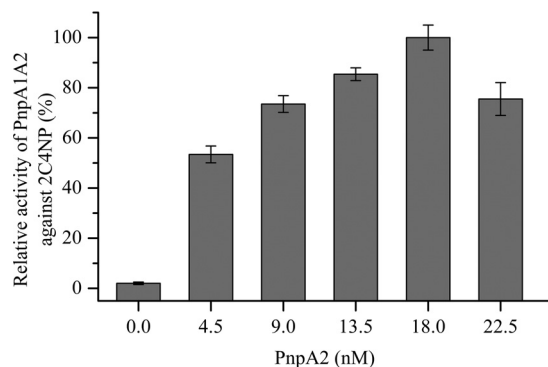
FIG 5 Relationship between the 2C4NP monooxygenase activity and various concentrations of H_6-PnpA2 while the concentration of H_6-PnpA1 was kept constant. The amount of H_6-PnpA2 was increased from 0 to 22.5 nM when the amount of H_6-PnpA1 was kept constant at 1 μM. The PnpA1 specific activity of 0.02 U mg^{-1} against 2C4NP was defined as 100% when 18 nM PnpA2 was added. The data are derived from three independent measurements, and error bars indicate standard deviations.
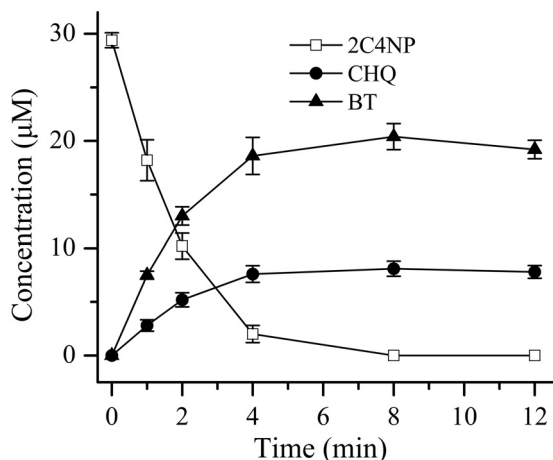
FIG 6 Time course of 2C4NP degradation by purified PnpA1A2. Ascorbic acid was added to the reaction mixture at a final concentration of 1 mM to reduce quinones to quinols. Samples were withdrawn at the indicated time points and treated immediately with glacial acetic acid (1%) to stop the reaction. The disappearance of 2C4NP and the appearance of the products (CHQ and BT) were quantified by HPLC. The experiments were performed in triplicate, the results shown are average values from three independent experiments, and error bars indicate standard deviations.

FIG 7 Whole-cell biotransformation of 2C4NP and PNP by RKJ300Δ$pnpA1$. Strain RKJ300Δ$pnpA1$ was grown on MM containing 0.2% (wt/vol) yeast extract to an OD_{600} of 0.3 and induced by 0.3 mM 2C4NP or PNP. Cells were harvested, and suspended to an OD_{600} of 2.0 in phosphate buffer containing 0.3 mM substrate (2C4NP or PNP). 4-NC, 4-nitrocatechol. All of the experiments were performed in triplicate, the results shown are average values from three independent experiments, and error bars indicate standard deviations.

mM ascorbic acid was added into the reaction mixture to minimize the autoxidation of the products. By HPLC and GC-MS analyses, both CHQ and BT were identified as products of 2C4NP monooxygenation in the system containing purified PnpA1A2. In a time course assay of monooxygenation reaction, 2C4NP consumption (29.4 μM) was approximately equivalent to the total accumulation of both CHQ (7.8 μM) and BT (19.2 μM) (Fig. 6), indicating a nearly stoichiometric formation of CHQ and BT from 2C4NP. Similarly, HQ and BT were identified as the products of PNP catalyzed by purified PnpA1A2.

(v) PnpA1A2 catalyzes a poor conversion of CHQ and HQ to BT. Generally, most of the members of the phenol 4-monooxygenase group of the TC-FDM family were proposed to hydroxylate their substrates twice in tandem (17). Therefore, CHQ and HQ were also used as the initial substrates to see whether the purified PnpA1A2 can catalyze the hydroxylation of these two compounds. Although with low conversion rates (less than 0.0002 U mg^{-1}), by GC-MS analysis, PnpA1A2 was found to also be able to catalyze the hydroxylation of CHQ and HQ to produce BT (see Fig. S3 in the supplemental material), a likely ring cleavage substrate during the degradation of 2C4NP and PNP in this strain.

***pnpA1* is essential for strain RKJ300 to utilize 2C4NP.** To investigate the physiological roles of the two-component monooxygenase (PnpA1A2) in 2C4NP and PNP catabolism *in vivo*, derivatives of strain RKJ300 with deletion of the encoding gene of the oxidase component (PnpA1) were constructed. Strain RKJ300Δ*pnpA1* (with *pnpA1* deleted) completely lost its ability to grow on 2C4NP as well as PNP, and *pnpA1*-complemented mutant RKJ300Δ*pnpA1*[pRESQ-*pnpA1*] regained its ability to grow on these two substrates. This clearly revealed that *pnpA1* was absolutely essential for strain RKJ300 to utilize 2C4NP and PNP as the sole sources of carbon and energy. Interestingly, in the biotransformation assay, strain RKJ300Δ*pnpA1* is unable to degrade 2C4NP, but it can transform PNP (yellow) slowly into a yellow-orange compound (with an approximate conversion rate

of 6.5 μM/OD_{600} of cell/h) (Fig. 7). The yellow-orange compound was identified as 4-nitrocatechol by HPLC analysis, and it was not degraded further even after a longer incubation period. These findings indicated that there is another enzyme involved in PNP transformation in strain RKJ300, in addition to PnpA1.

DISCUSSION

To date, two typical HQ ring cleavage enzymes, including the LinE-like single-subunit HQ dioxygenase (41, 42) and the HapCD-like two-subunit HQ dioxygenase (14, 35, 43), have been reported in bacterial catabolism of aromatics. Previously, strain RKJ300 was reported to degrade 2C4NP with initial formation of CHQ, which was further degraded via an HQ pathway (Fig. 8B) (4), but with no genetic and enzymatic evidence. In this study, the gene(s) encoding the potential LinE- or HapCD-like HQ dioxygenase was not found from its draft genome by initial bioinformatic analysis. Subsequent biochemical and genetic analyses demonstrated that the 2C4NP catabolism in strain RKJ300 was via the BT pathway rather than the reported HQ pathway, filling a gap in our knowledge of the 2C4NP degradation mechanism at the molecular and biochemical levels in Gram-positive bacteria.

The 2C4NP catabolic pathway identified in strain RKJ300 is significantly different from those of the other three reported 2C4NP utilizers. In the previous studies of 2C4NP catabolism, CHQ was identified as the ring cleavage substrate in *Burkholderia* sp. strain SJ98 (Fig. 8C) (14) and *Arthrobacter* sp. strain SJCon (Fig. 8D) (5). The identification of BT as the ring cleavage substrate in the present study (Fig. 8A) clearly indicates that the chloro group was removed before ring cleavage during 2C4NP catabolism in strain RKJ300, whereas this removal occurs after ring cleavage in the above two 2C4NP degraders (5, 14). Although the chloro group in 2C4NP degradation by the utilizer *Burkholderia* sp. strain RKJ 800 was also removed before ring cleavage, the ring cleavage substrate was HQ (Fig. 8B) (3) rather than BT. It can be concluded that the 2C4NP degradation via the BT pathway in strain RKJ300 reveals a novel catabolic pathway that was not previously reported for 2C4NP catabolism.
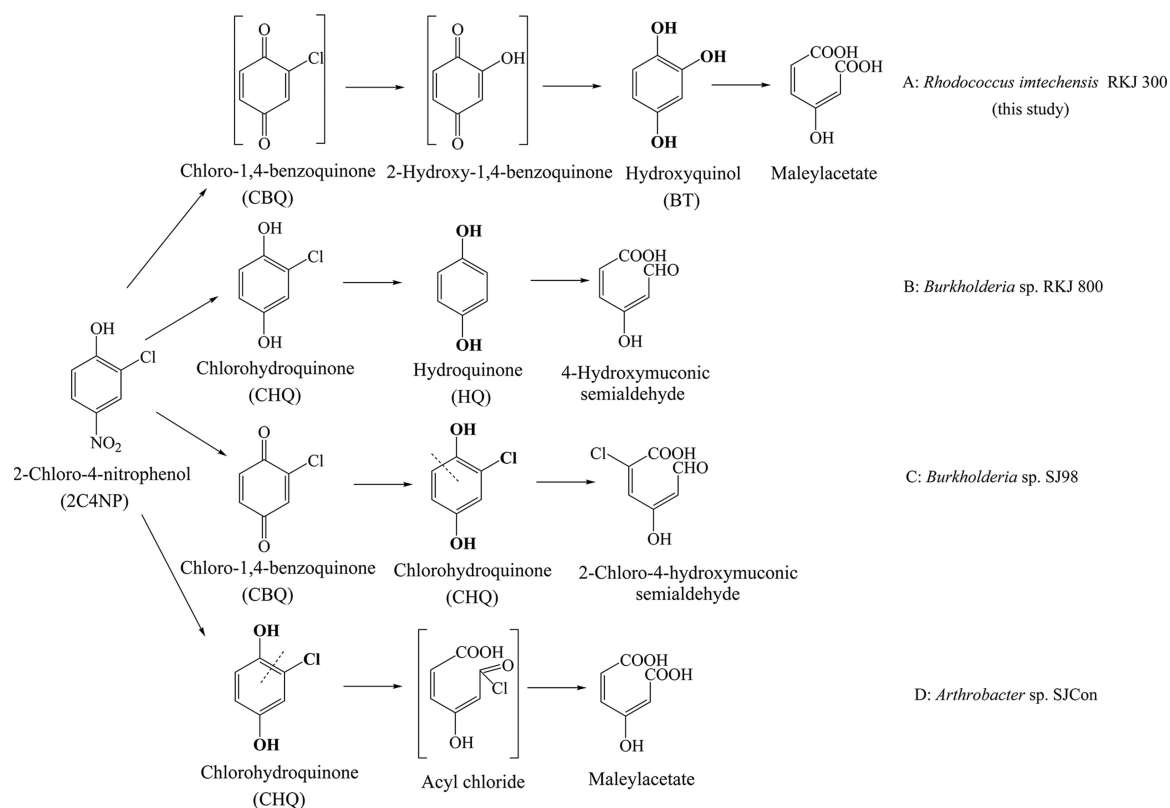
FIG 8 Proposed pathways of 2C4NP degradation by different 2C4NP utilizers. (A) *R. imtechensis* strain RKJ300 (this study). (B) *Burkholderia* sp. strain RKJ800 (3) (this pathway was also seen with *R. imtechensis* strain RKJ300, reported previously [4]). (C) *Burkholderia* sp. strain SJ98 (14). (D) *Arthrobacter* sp. strain SJCon (5). The unidentified intermediates are in brackets. The structures of ring cleavage compounds are indicated in boldface, and the dashed lines in panels C and D indicate the ring cleavage positions.

Recently, the molecular mechanism of 2C4NP degradation was reported in Gram-negative *Burkholderia* sp. strain SJ98 (14). However, no such information has been reported in Gram-positive bacteria, although two Gram-positive 2C4NP utilizers (4, 5) were isolated. In this study, the high transcription of the *pnp* cluster in 2C4NP- and PNP-induced cells indicated that the enzymes encoded by the *pnp* genes were likely involved in both 2C4NP catabolism and PNP catabolism in strain RKJ300. Enzymatic assay and identification of intermediates have shown that PnpA1A2 has the ability to catalyze the oxidation of both 2C4NP and PNP to BT, and *pnpA1* is necessary for strain RKJ300 to utilize 2C4NP and PNP. Considering the significant increase in the transcriptional levels of *pnpB* and *pnpC* under 2C4NP- and PNP-induced conditions, it is reasonable to conclude that PnpB and PnpC are likely responsible for the BT ring cleavage and the maleylacetate reduction, respectively, in the lower pathway of the catabolism of both 2C4NP and PNP in strain RKJ300 (Fig. 3C). On the other hand, PnpA1A2-initiated 2C4NP catabolism clearly indicated that the molecular mechanism of 2C4NP degradation in Gram-positive strain RKJ300 is different from that previously reported in Gram-negative *Burkholderia* sp. strain SJ98 where a single-component PNP 4-monooxygenase PnpA was proven to initiate 2C4NP degradation (14).

It is generally accepted that a monooxygenase attack on an aromatic ring at a position occupied by an electron-withdrawing group (such as a chloro or nitro group) produces a quinone (14, 17, 44, 45), while an attack at an unsubstituted position produces

a quinol (46, 47). Therefore, the detection of CHQ from the PnpA1A2-catalyzed 2C4NP conversion proposed that chloro-1,4-benzoquinone (CBQ) was the direct product (Fig. 3C). The production of CHQ during 2C4NP degradation is probably due to the nonenzymatic reduction of CBQ by small reducing agents, such as NADH or ascorbic acid, and the same explanations were also proposed previously for PNP (9) and 2,4,6-trichlorophenol (45) degradation. On the other hand, the conversion of CHQ to BT by PnpA1A2 could eliminate the toxicity of CHQ against strain RKJ300, and this also revealed the probable fate of the by-product CHQ during 2C4NP degradation.

Most members of the phenol 4-monooxygenase group of the TC-FDM family were reported to hydroxylate their substrates twice in tandem (17, 38, 45, 48). Therefore, the identification of BT as the preponderant product of 2C4NP by PnpA1A2 presents strong evidence that CBQ from the first catalytic step would be further hydrolyzed to BT via 2-hydroxy-1,4-benzoquinone. According to this study, we concluded that PnpA1A2 converts 2C4NP to BT by means of two different reactions: (i) it oxidizes 2C4NP to CBQ, and then (ii) it hydrolyzes CBQ to BT (Fig. 3C). Although PnpA1A2 has the ability to catalyze CHQ to BT, the extremely low rate of reaction suggested that the conversion of CHQ to BT was not likely the main pathway of 2C4NP catabolism in strain RKJ300 (Fig. 3C). The sequential process of denitration and dechlorination of 2C4NP by PnpA1A2 is very similar to the catalytic mechanism of TcpA, a homolog of PnpA1, against 2,4,6-trichlorophenol during 2,4,6-TCP degradation by *Ralstonia eutro-*

pha JMP134. TcpA was reported to catalyze the sequential dechlorinations of 2,4,6-trichlorophenol to 6-chlorohydroxyquinol via 2,6-dichloroquinone and 6-chlorohydroxyquinone (45).

For PNP catabolism, it was generally accepted that BT is the ring cleavage substrate in Gram-positive strains (11, 12, 17, 18, 41, 48), while HQ is the ring cleavage substrate in Gram-negative bacteria (9, 14, 49–51). Interestingly, a small amount of HQ has been detected during PNP catabolism in most Gram-positive strains (12, 17, 18, 38); however, the fate of HQ remains unclear. In this study, HQ was also detected during PNP catabolism by strain RKJ300. Intriguingly, PnpA1A2 was found to be able to catalyze the conversion of HQ to BT (although with a low specific activity), indicating that the produced HQ during PNP catabolism in Gram-positive PNP utilizers could be likely further degraded via the existing BT pathway.

ACKNOWLEDGMENTS

REFERENCES

1. **Arora PK, Sasikala C, Ramana CV.** 2012. Degradation of chlorinated nitroaromatic compounds. Appl Microbiol Biotechnol **93:**2265–2277. http://dx.doi.org/10.1007/s00253-012-3927-1.
2. **Pandey J, Heipieper HJ, Chauhan A, Arora PK, Prakash D, Takeo M, Jain RK.** 2011. Reductive dehalogenation mediated initiation of aerobic degradation of 2-chloro-4-nitrophenol by *Burkholderia* sp. strain SJ98. Appl Microbiol Biotechnol **92:**597–607. http://dx.doi.org/10.1007/s00253-011-3254-y.
3. **Arora PK, Jain RK.** 2012. Metabolism of 2-chloro-4-nitrophenol in a Gram negative bacterium, *Burkholderia* sp. RKJ 800. PLoS One **7:**e38676. http://dx.doi.org/10.1371/journal.pone.0038676.
4. **Ghosh A, Khurana M, Chauhan A, Takeo M, Chakraborti AK, Jain RK.** 2010. Degradation of 4-nitrophenol, 2-chloro-4-nitrophenol, and 2,4-dinitrophenol by *Rhodococcus imtechensis* strain RKJ300. Environ Sci Technol **44:**1069–1077. http://dx.doi.org/10.1021/es9034123.
5. **Arora PK, Jain RK.** 2011. Pathway for degradation of 2-chloro-4-nitrophenol in *Arthrobacter* sp. SJCon. Curr Microbiol **63:**568–573. http://dx.doi.org/10.1007/s00284-011-0022-2.
6. **Arora PK, Sharma A, Mehta R, Shenoy BD, Srivastava A, Singh VP.** 2012. Metabolism of 4-chloro-2-nitrophenol in a Gram-positive bacterium, *Exiguobacterium* sp. PMA. Microb Cell Fact **11:**150. http://dx.doi.org/10.1186/1475-2859-11-150.
7. **Schenzle A, Lenke H, Spain JC, Knackmuss HJ.** 1999. Chemoselective nitro group reduction and reductive dechlorination initiate degradation of 2-chloro-5-nitrophenol by *Ralstonia eutropha* JMP134. Appl Environ Microbiol **65:**2317–2323.
8. **Yin Y, Xiao Y, Liu HZ, Hao F, Rayner S, Tang H, Zhou NY.** 2010. Characterization of catabolic *meta*-nitrophenol nitroreductase from *Cupriavidus necator* JMP134. Appl Microbiol Biotechnol **87:**2077–2085. http://dx.doi.org/10.1007/s00253-010-2666-4.
9. **Zhang JJ, Liu H, Xiao Y, Zhang XE, Zhou NY.** 2009. Identification and characterization of catabolic *para*-nitrophenol 4-monooxygenase and *para*-benzoquinone reductase from *Pseudomonas* sp. strain WBC-3. J Bacteriol **191:**2703–2710. http://dx.doi.org/10.1128/JB.01566-08.
10. **Xiao Y, Zhang JJ, Liu H, Zhou NY.** 2007. Molecular characterization of a novel *ortho*-nitrophenol catabolic gene cluster in *Alcaligenes* sp. strain NyZ215. J Bacteriol **189:**6587–6593. http://dx.doi.org/10.1128/JB.00654-07.
11. **Kitagawa W, Kimura N, Kamagata Y.** 2004. A novel *p*-nitrophenol degradation gene cluster from a Gram-positive bacterium, Rhodococcus

12. opacus SAO101. J Bacteriol **186:**4894–4902. http://dx.doi.org/10.1128/JB.186.15.4894-4902.2004.
12. **Jain RK, Dreisbach JH, Spain JC.** 1994. Biodegradation of *p*-nitrophenol via 1,2,4-benzenetriol by an *Arthrobacter* sp. Appl Environ Microbiol **60:**3030–3032.
13. **Spain JC, Gibson DT.** 1991. Pathway for biodegradation of *p*-nitrophenol in a *Moraxella* sp. Appl Environ Microbiol **57:**812–819.
14. **Min J, Zhang JJ, Zhou NY.** 2014. The gene cluster for *para*-nitrophenol catabolism is responsible for 2-chloro-4-nitrophenol degradation in *Burkholderia* sp. strain SJ98. Appl Environ Microbiol **80:**6212–6222. http://dx.doi.org/10.1128/AEM.02093-14.
15. **Liu H, Wang SJ.** 2005. A new isolate of *Pseudomonas stutzeri* that degrades 2-chloronitrobenzene. Biotechnol Lett **27:**275–278. http://dx.doi.org/10.1007/s10529-004-8293-3.
16. **Chen YF, Chao H, Zhou NY.** 2014. The catabolism of 2,4-xylenol and *p*-cresol share the enzymes for the oxidation of *para*-methyl group in *Pseudomonas putida* NCIMB 9866. Appl Microbiol Biotechnol **98:**1349–1356. http://dx.doi.org/10.1007/s00253-013-5001-z.
17. **Perry LL, Zylstra GJ.** 2007. Cloning of a gene cluster involved in the catabolism of *p*-nitrophenol by *Arthrobacter* sp. strain JS443 and characterization of the *p*-nitrophenol monooxygenase. J Bacteriol **189:**7563–7572. http://dx.doi.org/10.1128/JB.01849-06.
18. **Liu PP, Zhang JJ, Zhou NY.** 2010. Characterization and mutagenesis of a two-component monooxygenase involved in *para*-nitrophenol degradation by an *Arthrobacter* strain. Int Biodeterior Biodegrad **64:**293–299. http://dx.doi.org/10.1016/j.ibiod.2010.03.001.
19. **Chao H, Zhou NY.** 2013. GenR, an IclR-type regulator, activates and represses the transcription of gen genes involved in 3-hydroxybenzoate and gentisate catabolism in *Corynebacterium glutamicum*. J Bacteriol **195:**1598–1609. http://dx.doi.org/10.1128/JB.02216-12.
20. **Livak KJ, Schmittgen TD.** 2001. Analysis of relative gene expression data using real-time quantitative PCR and the $2^{-\Delta\Delta C_T}$ method. Methods **25:**402–408. http://dx.doi.org/10.1006/meth.2001.1262.
21. **Liu TT, Zhou NY.** 2012. Novel L-cysteine-dependent maleylpyruvate isomerase in the gentisate pathway of *Paenibacillus* sp. strain NyZ101. J Bacteriol **194:**3987–3994. http://dx.doi.org/10.1128/JB.00050-12.
22. **Galán B, Díaz E, Prieto MA, Garcia JL.** 2000. Functional analysis of the small component of the 4-hydroxyphenylacetate 3-monooxygenase of *Escherichia coli* W: a prototype of a new flavin:NAD(P)H reductase subfamily. J Bacteriol **182:**627–636. http://dx.doi.org/10.1128/JB.182.3.627-636.2000.
23. **Fontecave M, Eliasson R, Reichard P.** 1987. NAD(P)H:flavin oxidoreductase of *Escherichia coli*. A ferric iron reductase participating in the generation of the free radical of ribonucleotide reductase. J Biol Chem **262:**12325–12331.
24. **Spain JC, Wyss O, Gibson DT.** 1979. Enzymatic oxidation of *p*-nitrophenol. Biochem Biophys Res Commun **88:**634–641. http://dx.doi.org/10.1016/0006-291X(79)92095-3.
25. **Winn-Deen ES, David H, Sigler G, Chavez R.** 1988. Development of a direct assay for α-amylase. Clin Chem **34:**2005–2008.
26. **Louie TM, Webster CM, Xun L.** 2002. Genetic and biochemical characterization of a 2,4,6-trichlorophenol degradation pathway in *Ralstonia eutropha* JMP134. J Bacteriol **184:**3492–3500. http://dx.doi.org/10.1128/JB.184.13.3492-3500.2002.
27. **Bradford MM.** 1976. A rapid and sensitive method for the quantitation of microgram quantities of protein utilizing the principle of protein-dye binding. Anal Biochem **72:**248–254. http://dx.doi.org/10.1016/0003-2697(76)90527-3.
28. **Jakoby M, Ngouoto-Nkili CE, Burkovski A.** 1999. Construction and application of new *Corynebacterium glutamicum* vectors. Biotechnol Tech **13:**437–441. http://dx.doi.org/10.1023/A:1008968419217.
29. **Schafer A, Tauch A, Jager W, Kalinowski J, Thierbach G, Puhler A.** 1994. Small mobilizable multi-purpose cloning vectors derived from the *Escherichia coli* plasmids pK18 and pK19: selection of defined deletions in the chromosome of *Corynebacterium glutamicum*. Gene **145:**69–73. http://dx.doi.org/10.1016/0378-1119(94)90324-7.
30. **Simon R, Priefer U, Puhler A.** 1983. A broad host range mobilization system for in vivo genetic engineering: transposon mutagenesis in Gram-negative bacteria. Biotechnology (NY) **1:**784–791. http://dx.doi.org/10.1038/nbt1183-784.
31. **Saltikov CW, Newman DK.** 2003. Genetic identification of a respiratory arsenate reductase. Proc Natl Acad Sci U S A **100:**10983–10988. http://dx.doi.org/10.1073/pnas.1834303100.

32. **van der Geize RHG, van Gerwen R, van der Meijden P, Dijkhuizen L.** 2002. Molecular and functional characterization of *kshA* and *kshB*, encoding two components of 3-ketosteroid 9a-hydroxylase, a class IA monooxygenase, in *Rhodococcus erythropolis* strain SQ1. Mol Microbiol **45**:1007–1018. http://dx.doi.org/10.1046/j.1365-2958.2002.03069.x.

33. **van der Geize R, Hessels GI, van Gerwen R, Vrijbloed JW, van der Meijden P, Dijkhuizen L.** 2000. Targeted disruption of the *kstD* gene encoding a 3-ketosteroid Δ^1-dehydrogenase isoenzyme of *Rhodococcus erythropolis* strain SQ1. Appl Environ Microbiol **66**:2029–2036. http://dx.doi.org/10.1128/AEM.66.5.2029-2036.2000.

34. **Chapman PJ, Hopper DJ.** 1968. The bacterial metabolism of 2,4-xylenol. Biochem J **110**:491–498. http://dx.doi.org/10.1042/bj1100491.

35. **Moonen MJ, Synowsky SA, van den Berg WA, Westphal AH, Heck AJ, van den Heuvel RH, Fraaije MW, van Berkel WJ.** 2008. Hydroquinone dioxygenase from *Pseudomonas fluorescens* ACB: a novel member of the family of nonheme-iron(II)-dependent dioxygenases. J Bacteriol **190**:5199–5209. http://dx.doi.org/10.1128/JB.01945-07.

36. **Ferreira MI, Marchesi JR, Janssen DB.** 2008. Degradation of 4-fluorophenol by *Arthrobacter* sp. strain IF1. Appl Microbiol Biotechnol **78**:709–717. http://dx.doi.org/10.1007/s00253-008-1343-3.

37. **Vikram S, Kumar S, Subramanian S, Raghava GPS.** 2012. Draft genome sequence of the nitrophenol-degrading actinomycete *Rhodococcus imtechensis* RKJ300. J Bacteriol **194**:3543–3543. http://dx.doi.org/10.1128/JB.00532-12.

38. **Yamamoto K, Nishimura M, Kato D, Takeo M, Negoro S.** 2011. Identification and characterization of another 4-nitrophenol degradation gene cluster, nps, in Rhodococcus sp. strain PN1. J Biosci Bioeng **111**:687–694. http://dx.doi.org/10.1016/j.jbiosc.2011.01.016.

39. **Coves J, Niviere V, Eschenbrenner M, Fontecave M.** 1993. NADPH-sulfite reductase from *Escherichia coli*—a flavin reductase participating in the generation of the free-radical of ribonucleotide reductase. J Biol Chem **268**:18604–18609.

40. **Takeo MYT, Abe Y, Niihara S, Maeda Y, Negoro S.** 2003. Cloning and characterization of a 4-nitrophenol hydroxylase gene cluster from *Rhodococcus* sp. PN1. J Biosci Bioeng **95**:139–145. http://dx.doi.org/10.1016/S1389-1723(03)80119-6.

41. **Ohtsubo Y, Miyauchi K, Kanda K, Hatta T, Kiyohara H, Senda T, Nagata Y, Mitsui Y, Takagi M.** 1999. PcpA, which is involved in the degradation of pentachlorophenol in *Sphingomonas chlorophenolica* ATCC39723, is a novel type of ring-cleavage dioxygenase. FEBS Lett **459**:395–398. http://dx.doi.org/10.1016/S0014-5793(99)01305-8.

42. **Miyauchi K, Adachi Y, Nagata Y, Takagi M.** 1999. Cloning and sequencing of a novel *meta*-cleavage dioxygenase gene whose product is involved in degradation of γ-hexachlorocyclohexane in *Sphingomonas paucimobilis*. J Bacteriol **181**:6712–6719.

43. **Vikram S, Pandey J, Bhalla N, Pandey G, Ghosh A, Khan F, Jain RK, Raghava GP.** 2012. Branching of the *p*-nitrophenol (PNP) degradation pathway in *Burkholderia* sp. strain SJ98: evidences from genetic characterization of PNP gene cluster. AMB Express **2**:30. http://dx.doi.org/10.1186/2191-0855-2-30.

44. **Haigler BE, Suen WC, Spain JC.** 1996. Purification and sequence analysis of 4-methyl-5-nitrocatechol oxygenase from *Burkholderia* sp. strain DNT. J Bacteriol **178**:6019–6024.

45. **Xun L, Webster CM.** 2004. A monooxygenase catalyzes sequential dechlorinations of 2,4,6-trichlorophenol by oxidative and hydrolytic reactions. J Biol Chem **279**:6696–6700.

46. **Whited GM, Gibson DT.** 1991. Toluene-4-monooxygenase, a three-component enzyme system that catalyzes the oxidation of toluene to *p*-cresol in *Pseudomonas mendocina* KR1. J Bacteriol **173**:3010–3016.

47. **Tao Y, Fishman A, Bentley WE, Wood TK.** 2004. Oxidation of benzene to phenol, catechol, and 1,2,3-trihydroxybenzene by toluene 4-monooxygenase of *Pseudomonas mendocina* KR1 and toluene 3-monooxygenase of *Ralstonia pickettii* PKO1. Appl Environ Microbiol **70**:3814–3820. http://dx.doi.org/10.1128/AEM.70.7.3814-3820.2004.

48. **Kadiyala V, Spain JC.** 1998. A two-component monooxygenase catalyzes both the hydroxylation of *p*-nitrophenol and the oxidative release of nitrite from 4-nitrocatechol in *Bacillus sphaericus* JS905. Appl Environ Microbiol **64**:2479–2484.

49. **Zhang S, Sun W, Xu L, Zheng X, Chu X, Tian J, Wu N, Fan Y.** 2012. Identification of the *para*-nitrophenol catabolic pathway, and characterization of three enzymes involved in the hydroquinone pathway, in *Pseudomonas* sp. 1-7. BMC Microbiol **12**:27. http://dx.doi.org/10.1186/1471-2180-12-27.

50. **Wei Q, Liu H, Zhang JJ, Wang SH, Xiao Y, Zhou NY.** 2010. Characterization of a *para*-nitrophenol catabolic cluster in *Pseudomonas* sp. strain NyZ402 and construction of an engineered strain capable of simultaneously mineralizing both *para*- and *ortho*-nitrophenols. Biodegradation **21**:575–584. http://dx.doi.org/10.1007/s10532-009-9325-4.

51. **Shen W, Liu W, Zhang J, Tao J, Deng H, Cao H, Cui Z.** 2010. Cloning and characterization of a gene cluster involved in the catabolism of *p*-nitrophenol from *Pseudomonas putida* DLL-E4. Bioresour Technol **101**:7516–7522. http://dx.doi.org/10.1016/j.biortech.2010.04.052.